The Amplitude and Time Course of the Myoplasmic Free [Ca^{2+}] Transient in Fast-twitch Fibers of Mouse Muscle

S. HOLLINGWORTH, MINGDI ZHAO, and S.M. BAYLOR

From the Department of Physiology, University of Pennsylvania School of Medicine, Philadelphia, Pennsylvania 19104-6085

ABSTRACT Bundles of 10–100 fibers were dissected from the extensor digitorum longus muscle of mouse, mounted in an apparatus for optical recording, and stretched to long sarcomere length (≥ 3.6 μm). One fiber within the bundle was microinjected with furaptra, a fluorescent indicator that responds rapidly to changes in myoplasmic free [Ca^{2+}] ($\Delta[Ca^{2+}]$). Twitches and brief tetani were initiated by external stimulation. At myoplasmic furaptra concentrations of ~0.1 mM, the indicator's fluorescence signal during fiber activity ($\Delta F/F$) was well resolved. $\Delta F/F$ was converted to $\Delta[Ca^{2+}]$ under the assumption that furaptra's myoplasmic dissociation constant for Ca^{2+} is 98 μM at 16°C and 109 μM at 28°C. At 16°C, the peak amplitude of $\Delta[Ca^{2+}]$ during a twitch was 17.8 ± 0.4 μM (±SEM; $n = 8$) and the half-width of $\Delta[Ca^{2+}]$ was 4.6 ± 0.3 ms. At 28°C, the peak and half-width values were 22.1 ± 1.8 μM and 2.0 ± 0.1 ms, respectively ($n = 4$). During a brief high-frequency tetanus, individual peaks of $\Delta[Ca^{2+}]$ were also well resolved and reached approximately the same amplitude that resulted from a single shock; the initial decays of $\Delta[Ca^{2+}]$ from peak slowed substantially during the tetanus. For a single twitch at 16°C, the amplitude of $\Delta[Ca^{2+}]$ in fast-twitch fibers of mouse is not significantly different from that recently measured in fast-twitch fibers of frog (16.5 ± 0.9 μM; Zhao, M., S. Hollingworth, and S.M. Baylor. 1996. *Biophys. J.* 70:896–916); in contrast, the half-width of $\Delta[Ca^{2+}]$ is surprisingly brief in mouse fibers, only about half that measured in frog (9.6 ± 0.6 ms). The estimated peak rate at which Ca^{2+} is released from the sarcoplasmic reticulum in response to an action potential is also similar in mouse and frog, 140–150 μM/ms (16°C).

KEY WORDS: calcium transients • mammalian muscle • fast-twitch fibers • furaptra • calcium indicators

INTRODUCTION

The changes in myoplasmic free [Ca^{2+}] ($\Delta[Ca^{2+}]$) that accompany activation of amphibian single muscle fibers have been widely studied with optical techniques. Less widely studied are $\Delta[Ca^{2+}]$ signals from single mammalian fibers, which are of smaller diameter and more easily damaged during muscle dissection. Two preparations, however, have given information about the amplitude of $\Delta[Ca^{2+}]$ in intact, fast-twitch mammalian fibers. In a singly dissected preparation from flexor digitorum brevis (FDB)[1] of mouse, the value of $\Delta[Ca^{2+}]$ during a brief high-frequency tetanus generally approached ~1 μM (22°C, measured with indo-1 and fura-2; Westerblad and Allen, 1991, 1993*a*, 1993*b*; Westerblad et al. 1993; Westerblad and Allen, 1994, 1996). A similar amplitude for tetanic $\Delta[Ca^{2+}]$, 0.2–2 μM, has been reported for enzymatically dissociated FDB fibers of rat (28–30°C, measured with fura-2; Carroll et al., 1995*a*; see, Figs. 5 and 7).

Several lines of evidence suggest that these estimates of tetanic [Ca^{2+}] in fast-twitch fibers of mammals may be too low. First, in intact fibers, maximal tetanic tension (~390 kNewtons/m^2, 25°C; Lannergren and Westerblad, 1987) is similar to the saturating level of tension measured in skinned fibers (~400 kN/m^2, 35°C; Stephenson and Williams, 1981); yet, in skinned fibers at 20–30°C, a 1 μM [Ca^{2+}] level generally produces half or less of the maximal Ca^{2+}-activated tension (Stephenson and Williams, 1981; Zot et al., 1986; Goldman et al., 1987; Godt and Nosek, 1989; Metzger and Moss, 1990). Also, in biochemical measurements of troponin reconstituted on the thin filament, the two Ca^{2+}-regulatory sites are reported to have dissociation constants for Ca^{2+} of 1–1.5 μM (rabbit troponin at 25°C; Zot and Potter, 1987). Since there appears to be a requirement that both sites bind Ca^{2+} for troponin to activate (e.g., Zot et al., 1986), tetanic [Ca^{2+}] levels of ~1 μM would again not appear capable of producing full activation in the intact fiber.

Second, in fast-twitch fibers of frog, peak values of $\Delta[Ca^{2+}]$ during a single twitch are reported to be large, ~17 μM for intact fibers (estimated with furaptra; Zhao et al., 1996) and 21-26 μM for cut fibers (estimated with purpurate-3,3′diacetic acid [PDAA]; Hirotaet al., 1989); similar peak values are also observed during a brief, high-frequency tetanus. One might have expected that the amplitude of Ca^{2+} transients in fast-twitch fibers of mammals would also be large, since

Address correspondence to Dr. S.M. Baylor, Department of Physiology, University of Pennsylvania School of Medicine, B-400 Richards Building, Philadelphia, PA 19104-6085. Fax: 215-573-5851; E-mail: baylor@mail.med.upenn.edu

[1]*Abbreviations used in this paper:* EDL, extensor digitorum longus; FDB, flexor digitorum brevis; SR, sarcoplasmic reticulum.

skinned-fiber tension-pCa relationships are generally similar for mammals and amphibians if measured in the same laboratory (e.g., Godt and Nosek, 1989, for rabbit; Maughan et al., 1995, for frog).

The low values reported for tetanic $[Ca^{2+}]$ in intact mammalian fibers might indicate that the tension-pCa relationship is more sensitive to $[Ca^{2+}]$ in intact compared with skinned fibers (Westerblad and Allen, 1996); however, it is also possible that the reported $[Ca^{2+}]$ levels are artifactually low because of indicator calibration problems. Both indo-1 and fura-2 are high-affinity indicators, and both bind heavily to myoplasmic constituents (Baylor and Hollingworth, 1988; Hove-Madsen and Bers, 1992; Baker et al., 1994; Zhao et al., 1996). As argued elsewhere (e.g., Konishi et al., 1988; Hirota et al., 1989; Kurebayashi et al., 1993; Zhao et al., 1996), heavily bound high-affinity indicators may substantially underestimate the actual level of $[Ca^{2+}]$. This possibility appears to be supported by the experiments of Delbono and Stefani (1993), who measured $\Delta[Ca^{2+}]$ in cut rat fibers with furaptra, a lower-affinity indicator that binds less heavily to myoplasmic constituents. The reported peak amplitude of $\Delta[Ca^{2+}]$ at 17°C was 4.6 ± 0.4 μM during a single twitch and 10.5 ± 1.3 μM during a brief voltage-clamp step (e.g., a 75-ms pulse to +20 mV). These measurements with furaptra in cut fibers suggest that $\Delta[Ca^{2+}]$ in intact mammalian fibers might rise well above the 1 μM level under physiological conditions.

To resolve this issue, we have used furaptra to estimate $\Delta[Ca^{2+}]$ during twitch and tetanus in intact extensor digitorum longus (EDL) fibers of mouse. The results indicate that the amplitude of $\Delta[Ca^{2+}]$ in fast-twitch fibers of mouse is indeed large: 17.8 ± 0.4 μM during a single twitch at 16°C and 22.1 ± 1.8 μM for a twitch at 28°C. Similarly large peak values of $\Delta[Ca^{2+}]$ were observed during brief, high-frequency tetani. The average value we report for peak $\Delta[Ca^{2+}]$ during a twitch at 16°C is very similar to that recently measured in our laboratory in frog fibers (16.5 ± 0.9 μM, also measured with furaptra; Zhao et al., 1996). The time course of $\Delta[Ca^{2+}]$, however, is substantially briefer in mouse compared with frog. For example, at 16°C, the half-width of $\Delta[Ca^{2+}]$ during a mouse twitch is only 4.6 ± 0.3 ms, whereas in frog it is 9.6 ± 0.6 ms (Zhao et al., 1996). In the DISCUSSION, kinetic modeling is used to assess the implications of the large and brief $\Delta[Ca^{2+}]$ signal that we measure in fast-twitch mammalian fibers.

MATERIALS AND METHODS

The methods used were similar to those previously described for frog fibers (e.g., Konishi et al., 1991; Zhao et al., 1996). Mouse fibers were bathed in a mammalian Ringer's solution of the following composition (in mM): 150 NaCl, 2 KCl, 2 $CaCl_2$, 1 $MgCl_2$, 5 HEPES, with pH titrated to 7.4 (20°C).

Preparation of Fiber Bundles and Injection of Indicator

Male Balb-C mice (7–8 wk of age) were purchased from Charles River Laboratories (Wilmington, MA) and kept for up to 2 wk in University of Pennsylvania animal facilities. On the day of an experiment, a mouse was killed by rapid cervical disarticulation, and the EDL muscles from both legs were removed by gross dissection. One muscle was stored at 4°C in oxygenated Ringer solution for later use (up to 3 h later); the other muscle was used immediately for dissection of a bundle of 10–100 fibers suitable for mounting in the experimental chamber. No measurement differences were noted according to whether an experiment was carried out on a freshly dissected or a stored EDL muscle.

The fine dissection, which used a needle and forceps, proceeded in two stages and took a total of 30–40 min. First, the four distal tendons of EDL were freed from their encapsulating sheath, and the three shorter heads were successively separated as entire units from the remaining muscle mass. Then, the fourth head was pared until a small bundle of fibers (10–100) remained. During this process, care was taken to leave one edge of the bundle relatively untouched by the dissecting instruments (typically, the edge at the side opposite the insertion of the other three heads).

After completion of the fine dissection, a small platinum-wire loop was attached to each tendon end, and the bundle was mounted on a horizontal optical bench apparatus in a temperature-controlled chamber with quartz windows (Baylor and Oetliker, 1977). One platinum loop was attached to a fixed hook and the other was attached to an AE 801 tension transducer (Senso-Nor, Horten, Norway). To minimize movement artifacts in the optical traces, the bundle was stretched to a long sarcomere length (generally, ~3.6 μm at the start of an experiment) and lowered onto a pair of supporting pedestals. The bundle was oriented so that the fibers that had been least disturbed during the fine dissection were located nearest the microelectrode used for the injection of indicator. Furaptra (tetra-K^+ form; Molecular Probes Inc., Eugene, OR), which was dissolved in distilled water at a concentration of 10–30 mM, was then pressure injected into a single fiber.

Optical Recording Procedures

One of three interference filters (Omega Optical, Brattleboro, VT or Chroma Technology, Brattleboro, VT) was used to select the fluorescence excitation bands (λ_{ex}'s): 350 ± 5, 380 ± 5, or 410 ± 20 nm. For $\lambda_{ex} < 400$ nm, a 75 W xenon source (Photon Technology Inc., Princeton, NJ) was used; for $\lambda_{ex} > 400$ nm, a 100 W tungsten-halogen source was preferred because of its greater stability. To increase excitation intensities at $\lambda_{ex} < 400$ nm, our usual long-working-distance condensing objective was replaced with a similar objective that had a higher UV transmittance (Leitz #518075, 32x, N.A. 0.4, working distance 6 mm; E. Leitz Inc., Rockleigh, NJ). A single fluorescence emission filter of wide bandpass (470–590 nm; Chroma Technology) was positioned in front of the photodiode unit that monitored fluorescence intensity.

At $\lambda_{ex} < 400$ nm, the instability of the UV arc lamp introduced relatively slow, ~1%, intensity fluctuations in the optical measurements. To reduce the influence of these fluctuations, a dichroic mirror that reflected light of wavelength ≤430 nm (430DCLP; Chroma Technology) was inserted in the light path between the preparation and the emission filter. This mirror reflected transmitted light at λ_{ex}, which was focused onto a second photodiode unit. Fluctuations in the output of the UV lamp thus appeared as changes in intensity at the second photodiode, which were monitored during each sweep. In the analysis stage, a ratio correction

was applied that removed fluctuations common to the outputs of the two photodiode units. This correction was identical to that described in connection with Eqs. 1 and 2 of the next section, except that the intensity of the second photodiode was treated as $\Delta F_1/F_1$ and that of the first photodiode as $\Delta F_2/F_2$; the value of the parameter K was assumed to be 1,000, i.e., effectively infinite. This correction successfully removed the 1% fluctuations in $\Delta F/F$ due to instability of the UV source and was applied to all traces reported in RESULTS obtained at λ_{ex} = 350 nm or 380 nm.

Fluorescence intensity was recorded from a 300-μm length of fiber centered near the injection site. For each measurement, the prestimulus value of fluorescence (resting fluorescence, F) and the stimulus-induced change in fluorescence intensity (ΔF) were recorded. All reported F values were corrected for a constant intensity level not related to the presence of indicator. This component was measured in each experiment from a bundle region located 1.5–2.5 mm along the fiber from the injection site, where indicator concentration was negligible. For most measurements, the non–indicator-related intensity was a small fraction (≤ 0.2) of the indicator-related intensity.

Fibers were studied only if they gave an all-or-none ΔF response to a brief (0.5 ms) supra-threshold shock initiated locally by a pair of extracellular electrodes. To minimize movement of the bundle during fiber activity, the stimulus intensity was adjusted so as to be just above threshold for furaptra's signal from the injected fiber. The stimulation cathode was typically located ~1 mm from the site of optical recording; at 16°C, the propagation time for the action potential to reach the recording site was ~1 ms. Because fluorescence levels were typically small, they were usually recorded with a 1 Gohm feedback resistor in the current-to-voltage converter of the photodiode circuit. This resistor introduced into the recording of fluorescence changes a first-order delay of 1.8 ms, which was corrected as described in the next section of MATERIALS AND METHODS.

The total concentration of furaptra within the fiber at the measurement location ($[D_T]$) was estimated from F(410), the value of F measured with λ_{ex} = 410 nm. The scaling factor to relate F(410) to $[D_T]$ was determined by the method of Konishi et al. (1991), in a separate set of experiments on frog single fibers; this determination used 410 or 420 nm illumination and simultaneous measurements of fluorescence and absorbance changes during activity ($\Delta F/F$ and ΔA, respectively). The scaling factor determined for frog fibers was applied to mouse fibers after appropriate adjustment for the difference in fiber diameters. The values of $[D_T]$ so determined fell in the range, 0.04–0.13 mM (see column 3 of Table I). These concentrations are sufficiently small that $\Delta[Ca^{2+}]$ is not expected to be perturbed significantly by the calcium buffer capacity of the indicator (Konishi et al., 1991).

Ratio Fluorescence Measurements

In four of the eight experiments, the ratio technique of Zhao et al. (1996), which is an extension of the ratio technique of Grynkiewicz et al. (1985), was used to reduce the influence of movement artifacts in the fluorescence signals. These artifacts are presumed to have arisen because of a change in the number of indicator molecules within the optical field (fractional change denoted $\Delta N/N$). For this purpose, $\Delta F/F$ signals were recorded sequentially with two UV excitation wavelengths (λ_{ex} = 350 and 380 nm; traces denoted $\Delta F_1/F_1$ and $\Delta F_2/F_2$, respectively). A typical sequence recorded $\Delta F_1/F_1$, $\Delta F_2/F_2$, and $\Delta F_1/F_1$ in response to identical stimuli separated by 30–60 s. To increase signal-to-noise ratio, responses from several such runs were sometimes averaged. In the analysis stage, the averaged $\Delta F_1/F_1$ and $\Delta F_2/F_2$ responses were combined to yield the ratio-corrected version of the $\Delta F_2/F_2$ trace (denoted $\Delta F_2'/F_2$), calculated as:

$$\Delta F'_2/F_2 = \frac{-K(\Delta F_2/F_2 - \Delta F_1/F_1)}{(1 - K + \Delta F_2/F_2 - K\Delta F_1/F_1)}, \quad (1)$$

and the estimate of $\Delta N/N$, calculated as:

$$\Delta N/N = \frac{(\Delta F_2/F_2 - K\Delta F_1/F_1)}{(1 - K)}. \quad (2)$$

In Eqs. 1 and 2 (which are the same as Eqs. A9 and A10 of Zhao et al. 1996 after reversal of the roles of γ_1 and γ_2), K represents the constant ratio $(\Delta F_2/F_2)/(\Delta F_1/F_1)$ that results if ΔF_1 and ΔF_2 are due to $\Delta[Ca^{2+}]$ alone. This use of the ratio technique permits estimation of $\Delta N/N$ even if $\Delta F_1/F_1$ is measured at a Ca^{2+}-sensitive wavelength, and it also has the theoretical advantage that the ratio-corrected trace ($\Delta F_2'/F_2$) retains a linear proportionality to Δf_{CaD} (the change in the fraction of the indicator in the Ca^{2+}-bound form during fiber activity). Examples of the $\Delta F_2'/F_2$ and $\Delta N/N$ traces calculated with Eqs. 1 and 2 are given in Fig. 1 *B*.

K was estimated in the analysis of each run, from a linear fit of the $\Delta F_2/F_2$ trace by the $\Delta F_1/F_1$ trace up to about the time-to-peak of the $\Delta F_2/F_2$ trace, i.e., to about the time of onset of the movement artifact (cf. Zhao et al., 1996). As expected for a well behaved indicator, the values of K were approximately constant, both within one experiment and from one experiment to another. For example, for the ratio-corrected runs reported in Table I, the average value of K was 2.89 with a population standard deviation of 0.21 (n = 7).

One of two procedures was used in the analysis stage to correct the ΔF traces for the 1.8-ms delay introduced by the 1 Gohm feedback resistor used to record light intensity (cf., preceding section). The first procedure was simply to use a digital filter to exponentially lead the relevant traces by 1.8 ms. For example, this correction was used for all ΔF traces shown in Fig. 1 — both those that did not use the ratio correction (see Fig. 1 *A*) and those that did (see Fig. 1 *B*). With the ratio technique, however, signal-to-noise ratio was increased if the $\Delta N/N$ trace was first calculated from the $\Delta F/F$ traces without correction for the delay. $\Delta F_2/F_2$ was then corrected for the delay and $\Delta F_2'/F_2$ calculated from:

$$\Delta F'_2/F_2 = \frac{(\Delta F_2/F_2 - \Delta N/N)}{(1 + \Delta N/N)} \quad (3)$$

Eq. 3 follows directly from Eq. A7 of Zhao et al. (1996). This second procedure could often be used because the movement artifact was usually sufficiently slow that $\Delta N/N$ was not distorted by the 1.8-ms first-order filter. In such cases, $\Delta N/N$ calculated from either the corrected or uncorrected $\Delta F/F$ traces differed only in signal-to-noise ratio.

Calculation of Δf_{CaD} and $\Delta[Ca^{2+}]$

According to Zhao et al. (1996), multiplication of furaptra's $\Delta F/F$ obtained with λ_{ex} = 410 nm by the factor −1.073 converts the fluorescence trace to units of Δf_{CaD}. Since it was determined empirically that $\Delta F/F$ measured with λ_{ex} = 380 nm is 0.976 times that measured with λ_{ex} = 410 nm, $\Delta F/F$ at 380 nm may be scaled by the factor −1.100 to give Δf_{CaD}. Δf_{CaD} was converted to $\Delta[Ca^{2+}]$ by:

$$\Delta[Ca^{2+}] = K_D \times \Delta f_{CaD} / (1 - \Delta f_{CaD}). \quad (4)$$

This equation follows from the equilibrium equation for 1:1 binding between indicator and Ca^{2+}, since f_{CaD}, the fraction of furaptra in the Ca^{2+}-bound form at rest, is essentially zero. The myoplasmic value of K_D, the apparent dissociation constant of furaptra for Ca^{2+}, was assumed to be 89 μM at 7°C, 98 μM at 16°C, 109 μM at 28°C, and 116 μM at 35°C.

The value of K_D assumed at 16°C is based on the absolute disso-

ciation constant of furaptra for Ca^{2+} measured at this temperature in a simple salt solution (44 μM; Konishi et al., 1991) in combination with two factors that act to elevate K_D. (*a*) Approximately half of the furaptra molecules in myoplasm appear to be bound to myoplasmic constituents of large molecular weight (Konishi et al., 1991); by analogy with fura-2 (e.g., Konishi et al., 1988), this binding is estimated to increase K_D (the apparent dissociation constant of bound and free furaptra treated as a single population) by about a factor of 2 (see also Zhao et al., 1996). (*b*) In a resting fiber at 16°C, ~0.1 of the indicator is in the Mg^{2+}-bound form (Konishi, et al., 1993); thus K_D will be further increased by ~1.1-fold over that applicable to a Mg^{2+}-free solution. The temperature dependence for K_D was obtained by a linear fit to furaptra's K_D data reported for a simple salt solution (44 μM at 16°C, mentioned above; 53 μM at 37°C, Raju et al., 1989), in combination with the assumption that factors (*a*) and (*b*) above do not vary with temperature. The increase in K_D with temperature may, in fact, be underestimated, since furaptra's dissociation constant for Mg^{2+} is reported to be smaller at higher temperatures (5.3 mM at 16°C, Konishi et al., 1991; 1.5 mM at 37°C, Raju et al., 1989).

Tension Transients

Although Ca^{2+} transients were detected from a single fiber, force transients were recorded from the end of the bundle and thus arose from both the injected fiber and any other fibers that were activated by the external shock. The amplitude of the force transients varied between 1 and 30×10^{-5} Newtons for a single twitch (sarcomere lengths, 3.6–4.0 μm). For most experiments, the number of fibers that contributed to the force transients was probably small (1–10), but the actual number is not known. Thus, tension records shown in RESULTS have not been calibrated in absolute units; rather, for any particular experiment, the records within any one figure are always shown at the same gain. These waveforms can therefore be used to roughly assess the effect on tension of experimental maneuvers such as changes in sarcomere length, the temperature of the bath, or the number of stimulating pulses.

Statistics

Statistics pertaining to the optical measurements are reported as mean ± SEM. The statistical significance of a difference between means was evaluated with Student's two-tailed t test; the significance level was set at $P < 0.05$.

RESULTS

Estimation of Δf_{CaD} from Furaptra during Single Twitches at 16°C

Previous articles from this laboratory have described the measurement of $\Delta[Ca^{2+}]$ from intact, fast-twitch fibers of frog muscle by means of kinetically rapid, lower-affinity Ca^{2+} indicators (PDAA, furaptra, mag-indo-1 and others; e.g., Konishi and Baylor, 1991; Konishi et al., 1991; Zhao et al., 1996). In those experiments, movement artifacts in the optical traces during twitches and brief tetani were reduced to negligible levels by (*a*) use of single fibers, (*b*) stretch of the fibers to long sarcomere lengths (3.5–4.3 μm), and (*c*) placement of the fibers over a two-pedestal support system. Since the

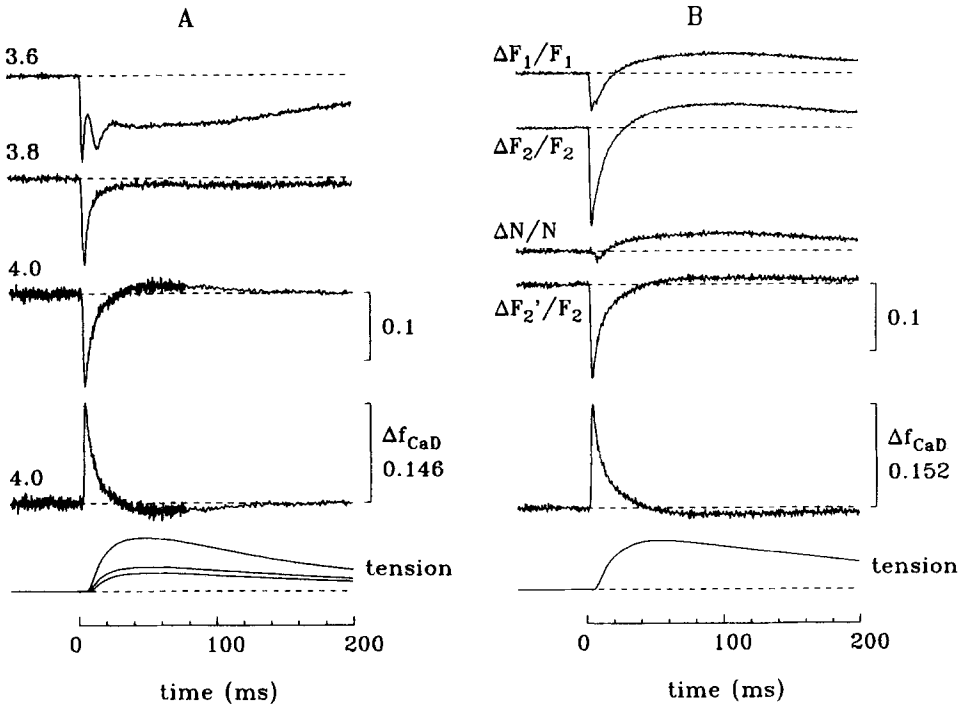

FIGURE 1. Examples from two experiments of furaptra-related optical signals (*upper traces*) and tension transients (*lowermost traces*) during single twitches. Zero time marks the moment of the external shock. (*A*) Fluorescence records (λ_{ex} = 410 nm) are shown at three different sarcomere length: 3.6, 3.8, and 4.0 μm (top three labeled traces); the calibration bar (units of $\Delta F/F$) applies to all three traces. The fourth trace (Δf_{CaD}) was obtained from the third trace by multiplication by the factor −1.073 (cf. MATERIALS AND METHODS). Fiber number, 032596.1; measurement times relative to the time of injection, 5, 14, and 29 min; estimated indicator concentrations, 91, 62, and 40 μM; fiber diameter, 48 μm (measured at a sarcomere length of 4.0 μm); number of stimuli per trace = 2 at each sarcomere length. (*B*) The upper two traces show fluorescence records (obtained with λ_{ex} = 350 and 380 nm, labeled $\Delta F_1/F_1$ and $\Delta F_2/F_2$, respectively), whereas the middle two traces (labeled $\Delta N/N$ and $\Delta F_2'/F_2$) were obtained from the upper two by Eqs. 1 and 2, as described in MATERIALS AND METHODS; the upper calibration bar applies to these four traces. The fifth trace (Δf_{CaD}) was obtained by multiplication of the $\Delta F_2'/F_2$ trace by the factor −1.100 (cf. MATERIALS AND METHODS). Fiber number, 040896.1; time after injection, 18–27 min; average indicator concentration, 117 μM; fiber diameter, 45 μm; sarcomere length, 3.8 μm; number of stimuli per trace: 6 ($\Delta F_1/F_1$), 3 ($\Delta F_2/F_2$).

present experiments used bundles of 10–100 mouse fibers, it was unclear at the outset whether movement artifacts could be reduced to the small levels characteristic of the frog experiments. First, bundles of mammalian fibers might be more susceptible to damage by stretch to long sarcomere lengths. Second, in our apparatus a fiber located near the top of a bundle presents the most convenient choice for injection with indicator; however, since the injected fiber does not rest directly on the pedestals, it may undergo greater movements than the fibers in contact with the pedestals. Thirdly, even with low stimulation voltages, non-injected fibers are sometimes activated, and their movement can contribute to optical artifacts. Our first experiments were therefore directed towards reduction of movement-related interference in the fluorescence records.

In the experiment of Fig. 1 *A*, a bundle was stretched to a relatively long sarcomere length (3.6 μm), a single fiber within the bundle was injected with furaptra, and the bundle was activated by a stimulus intensity that was just above threshold for the all-or-none optical response from the injected fiber. The upper three traces show the changes in furaptra's fluorescence measured at the initial sarcomere length (3.6 μm) and, later in the experiment, at two longer sarcomere lengths (3.8 and 4.0 μm; traces labeled accordingly). The lower superimposed traces show the associated tension transients; these became progressively smaller as sarcomere length was increased. The ΔF/F records, which were obtained with λ_{ex} = 410 nm, all reveal a well resolved, rapid decrease in fluorescence that begins shortly after stimulation and has a peak amplitude of ~−0.13. This signal undoubtedly reflects $\Delta[Ca^{2+}]$ (see below). The Ca^{2+}-related signal at 3.6 μm is followed by a substantial non-Ca^{2+} component (ΔF/F amplitude, ~−0.1) that, after an initial downward hump, returns slowly toward baseline during the remainder of the trace. This component is attributable to a movement artifact, since its amplitude was greatly reduced at the longer sarcomere lengths (3.8 and 4.0 μm) where the bundle's tension responses were substantially smaller. Small movement artifacts likely also contaminate the ΔF/F traces measured at 3.8 and 4.0 μm, since the later portions of these traces are not identical. Nevertheless, the principal characteristics of the early ΔF/F signal are very similar at 3.8 μm (peak amplitude, −0.128; half-width, 4.6 ms) and at 4.0 μm (peak amplitude, −0.136; half-width, 5.7 ms). Thus, in this fiber, the main characteristics of furaptra's Ca^{2+}-related signal appear to be well resolved by use of a single λ_{ex} and stretch of the bundle beyond 3.6 μm to reduce the movement artifact.

As described in MATERIALS AND METHODS, multiplication of furaptra's Ca^{2+} signal obtained at λ_{ex} = 410 nm by the scaling factor −1.073 converts this signal to Δf_{CaD} (the change in the fraction of the indicator in the Ca^{2+}-bound form). The fourth trace in Fig. 1 *A* shows the 4.0-μm trace so scaled; its values of peak amplitude (0.146), half-width (5.7 ms), and several other kinetic parameters are listed in part A of Table I (fiber 032596.1). The transient baseline undershoot observed after the early peak is likely to be a residual artifact of fiber movement.

TABLE I

Properties of Δf_{CaD} Measured with Furaptra during Single Twitches

(1)	(2)	(3)	(4)	(5)	(6)	(7)
			Δf_{CaD}			
Fiber reference	Fiber diameter	$[D_T]$	Time to half-rise	Time to peak	Half-width	Peak amplitude
	μm	μM	ms	ms	ms	
(A) 16°C						
032596.1	48	40	4.0	5.3	5.7	0.146
032596.2	45	80	2.9	4.0	4.7	0.154
040596.1	36	64	3.3	4.8	5.1	0.156
040596.2	51	99	3.1	4.5	4.7	0.167
040896.1*	45	117	3.0	4.0	6.4	0.152
040996.1*	33	99	2.2	3.0	4.4	0.153
040996.2*	39	125	3.5	4.8	6.7	0.156
040996.3*	(42)	113	2.9	4.0	3.7	0.141
Mean	42		3.1	4.3	5.2	0.153
SEM	3		0.2	0.3	0.4	0.003
(B) 28°C						
032596.2	45	46	1.3	1.8	1.8	0.180
040896.1*	51	67	1.6	2.0	2.5	0.175
040996.1*	33	99	1.2	2.0	2.2	0.135
040996.3*	(42)	85	1.5	2.0	2.1	0.184
Mean	43		1.4	2.0	2.2	0.169
SEM	5		0.1	0.1	0.1	0.011

Half-width is defined as the difference between the times to half-rise and half-decay. *Indicates measurements made with the ratio technique (cf. MATERIALS AND METHODS and Fig. 1 *B*); parentheses indicate that the information was not recorded and an average value was assumed. Sarcomere lengths fell in the range 3.8–4.1 μm.

A complementary strategy for reducing the movement artifact is to use the ratio technique (Grynkiewicz et al., 1985). This method introduces extra complexity, since it requires that fluorescence changes be recorded with two excitation wavelengths and/or two emission wavelengths. Fig. 1 *B* shows results obtained in another experiment, which used the ratio technique described in MATERIALS AND METHODS (Zhao et al., 1996); this technique allows estimation of a ratio-corrected trace that is linearly proportional to Δf_{CaD}. In the experiment of Fig. 1 *B*, the upper two traces (labeled $\Delta F_1/F_1$ and $\Delta F_2/F_2$) show fluorescence traces obtained with two excitation wavelengths (350 and 380 nm, respectively). Both of these traces contain a Ca^{2+}-related signal (the early decrease in fluorescence) and a movement-related signal (the delayed overshoot of the fluorescence baseline). These traces were combined (Eqs. 1

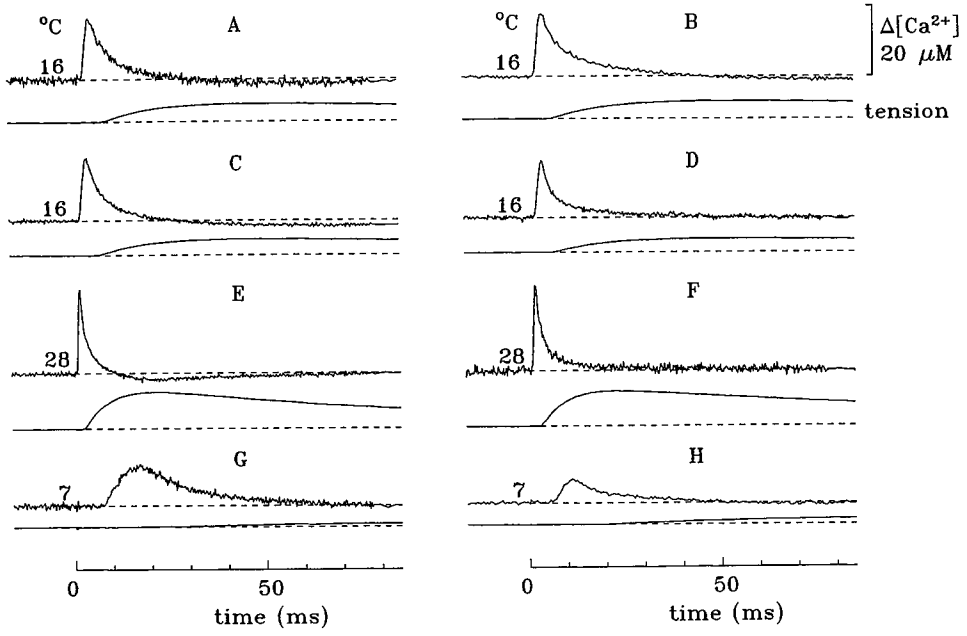

FIGURE 2. Examples of furaptra Ca^{2+} transients and tension in four experiments at 16°C (*A–D*), two experiments at 28°C (*E* and *F*), and two experiments at 7°C (*G* and *H*). Panels *A* and *B* are from the same experiments as *A* and *B* of Fig. 1; *C*, *E*, and *G* are from experiment 032596.2, with λ_{ex} = 410 nm only (as in Fig. 1 *A*); *D*, *F*, and *H* are from experiment 040996.3 and used the ratio technique (as in Fig. 1 *B*). The following values apply to fibers 032596.2 and 040996.3, respectively: times after injection, 16–55 and 17–60 min; indicator concentrations, 33–80 and 72–133 μM; sarcomere length, 3.8 μm and not measured; number of stimuli per trace, 2–3 and 3–4. For both fibers, the order of the measurements was 16, 28, 16, 7, and 16°C; $\Delta[Ca^{2+}]$ from the first measurement at 16°C is shown. For the bracketing measurements at 16°C, very similar time courses were observed; however, there was some difference in the peak amplitudes of $\Delta[Ca^{2+}]$. For fiber 032596.2, the 16°C amplitudes were 17.7, 17.6, and 17.2 μM; for fiber 040996.3, the amplitudes were 18.2, 17.6, and 13.7 μM.

and 2) to yield the third and fourth traces: $\Delta N/N$ (the estimated fractional change in the number of indicator molecules within the recording field) and $\Delta F_2'/F_2$ (the ratio-corrected version of the $\Delta F_2/F_2$ trace). If the ratio correction had worked perfectly, the $\Delta F_2'/F_2$ trace would be free of movement artifacts. A comparison of the $\Delta F_2/F_2$ and $\Delta F_2'/F_2$ waveforms, however, suggests that the ratio correction was only partially successful. Specifically, the delayed overshoot of the fluorescence baseline is reduced in the $\Delta F_2'/F_2$ trace but not eliminated. Because the fiber in this experiment was stretched to a long sarcomere length (3.8 μm), the parameters that describe the amplitude and early time course of the Ca^{2+} signal are not heavily influenced by use of the ratio technique; for example, peak and half-width values of the $\Delta F_2/F_2$ and $\Delta F_2'/F_2$ traces are −0.141 and −0.138, and 7.5 and 6.4 ms, respectively. Nevertheless, the ratio correction appears to supply a useful additional procedure for reducing the effects of fiber movement, and it was therefore used in the majority of the measurements (cf., fiber references in Table I marked with asterisks).

As described in MATERIALS AND METHODS, multiplication of furaptra's $\Delta F_2'/F_2$ trace (λ_{ex} = 380 nm) by the scaling factor −1.100 converts the waveform to Δf_{CaD}. The fifth trace in Fig. 1 *B* shows the Δf_{CaD} trace so obtained, and part A of Table I (fiber 040896.1) lists its values of peak amplitude (0.152), half-width (6.4 ms), and other kinetic parameters. These values are very similar to the corresponding values estimated for Δf_{CaD} in the experiment of Fig. 1 *A*. The later baseline undershoot in Fig. 1 *B* is again thought to reflect a movement artifact.

Results very similar to those illustrated in Fig. 1 were obtained in eight successful experiments. As indicated in part A of Table I (16°C), the average peak value of

TABLE II

Properties of $\Delta[Ca^{2+}]$ Measured with Furaptra during Single Twitches

(1)	(2)	(3)	(4)	(5)	(6)	(7)
			$\Delta[Ca^{2+}]$			
Temperature	Fiber diameter	*n*	Time to half-rise	Time to peak	Half-width	Peak amplitude
°C	μm		ms	ms	ms	μM
(A) Mouse						
16	33–51	8	3.2 ± 0.2	4.4 ± 0.2	4.6 ± 0.3	17.8 ± 0.4
28	33–51	4	1.4 ± 0.1	2.0 ± 0.1	2.0 ± 0.1	22.1 ± 1.8
(B) Frog						
16	69–114	12	3.1 ± 0.1	5.0 ± 0.1	9.6 ± 0.6	16.5 ± 0.9
16	45–51	3	2.7 ± 0.4	3.9 ± 0.6	8.6 ± 1.6	16.9 ± 1.5

Half-width is as defined in legend to Table I. $\Delta[Ca^{2+}]$ was calculated by Eq. 4 from the corresponding Δf_{CaD} signal; note that the transformation from Δf_{CaD} to $\Delta[Ca^{2+}]$ is slightly nonlinear. In A, results are summarized for the mouse experiments of this paper (cf. Table I). In B, the small-diameter frog results were obtained on the three frog experiments described in RESULTS, whereas the larger-diameter frog results were taken from the furaptra experiments of Zhao et al. (1996). Since Zhao et al. did not report all of the numbers in row 3 of this Table, their data were reanalyzed to obtain these numbers.

Δf_{CaD} was 0.153 ± 0.003 (± SEM), and the average values for time to half-rise, time to peak, and half-width of Δf_{CaD} were 3.1 ± 0.2, 4.3 ± 0.3, and 5.2 ± 0.4 ms, respectively. Interestingly, the amplitude of furaptra's Δf_{CaD} measured in mouse EDL fibers is not significantly different from that recently measured in fast-twitch fibers of frog muscle under very similar experimental conditions (0.142 ± 0.008; Zhao et al., 1996). The half-width of Δf_{CaD} in mouse, however, is only about half that measured in frog (10.9 ± 0.7 ms).

Properties of $\Delta[Ca^{2+}]$ Estimated with Furaptra

Given the assumption of an effective myoplasmic K_D of furaptra for Ca^{2+} (98 μM at 16°C; see MATERIALS AND METHODS), Eq. 4 permits conversion of furaptra's Δf_{CaD} signal to $\Delta[Ca^{2+}]$. Panels *A* and *B* of Fig. 2 show these conversions for the two experiments of Fig. 1 and panels *C* and *D* for two other fibers at 16°C. As expected from the small SEM values given in Table I, the appearance of these signals is remarkably similar among the various fibers. The main variation concerns the degree of overshoot or undershoot of the baseline at later times; this variation is likely due to the unpredictable influence of residual movement artifacts. (Note: in frog fibers in which movement artifacts have been essentially eliminated, $\Delta[Ca^{2+}]$ on the time scale of Fig. 2 returns close to, but remains elevated a few percent above, baseline [e.g., Konishi et al., 1991; Zhao et al., 1996]. We speculate that $\Delta[Ca^{2+}]$ in mouse fibers would behave similarly if measured in the absence of movement artifacts.) As given in Table II, the average values for peak and half-width of $\Delta[Ca^{2+}]$ at 16°C are 17.8 ± 0.4 μM and 4.6 ± 0.3 ms, respectively.

Temperature Dependence of $\Delta[Ca^{2+}]$ in a Twitch

In four experiments, $\Delta[Ca^{2+}]$ was measured at 16°C, then the temperature was changed to at least one other value (7°C, 28°C, and/or 35°C), and the measurement was repeated, and finally temperature was returned to 16°C, where a bracketing measurement was attempted. In two of the experiments (fibers 040996.3 and 032596.2) reasonably well bracketed responses were observed throughout the sequence of temperature changes (see legend of Fig. 2). Results from these experiments are shown in Fig. 2, *C–H* (16°C, *C* and *D*; 28°C, *E* and *F*; 7°C, *G* and *H*). In both experiments, the peak amplitude of $\Delta[Ca^{2+}]$ became larger with warming and smaller with cooling; as expected, the half-width of $\Delta[Ca^{2+}]$ decreased with warming and increased with cooling.

Fig. 3 plots the effect of temperature on the amplitude of $\Delta[Ca^{2+}]$ (*A*) and the half-width of $\Delta[Ca^{2+}]$ (*B*) for the four experiments with data at different temperatures. (Note: in fibers 040896.1 [×'s] and 040996.1 [+'s], optical responses measured at the warmer temperatures were all-or-none; however, on return to 16°C, neither fiber responded in an all-or-none fashion. Thus, temperature trends observed in the latter two fibers must be treated with caution.)

Tables I and II summarize information on the properties of Δf_{CaD} and $\Delta[Ca^{2+}]$ measured at 28°C. As expected, the average values of the kinetic parameters are all briefer at 28°C compared with 16°C. For example, the average half-width of $\Delta[Ca^{2+}]$ at 28°C (2.0 ± 0.1 ms) is less than half that observed at 16°C (4.6 ± 0.3 ms). For the single measurement at 35°C, the half-width of $\Delta[Ca^{2+}]$ was 1.5 ms.

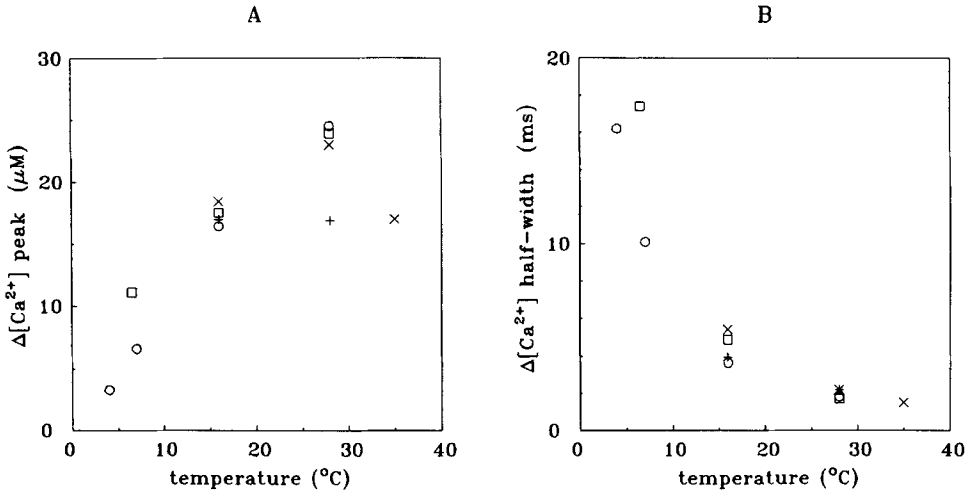

FIGURE 3. Effect of temperature on the peak amplitude (*A*) and the half-width (*B*) of furaptra Ca^{2+} signals measured during single twitches (*circles*, fiber 040996.3; *squares*, 032596.2; ×'s, 040896.1; +'s, 040996.1). For each experiment, the value shown at 16°C represents the average of all responses measured at that temperature during the runs. For these measurements, the following ranges apply: times after injection, 5–60 min; indicator concentrations, 33–117 μM; fiber diameters, 45–48 μm; sarcomere length, 3.8–3.9 μm; number of stimuli per trace, 1–5. Open symbols came from experiments in which all measurements were well bracketed upon final return to 16°C. In fiber 040896.1, data were obtained at 16°C, then 28°C, then 35°C.

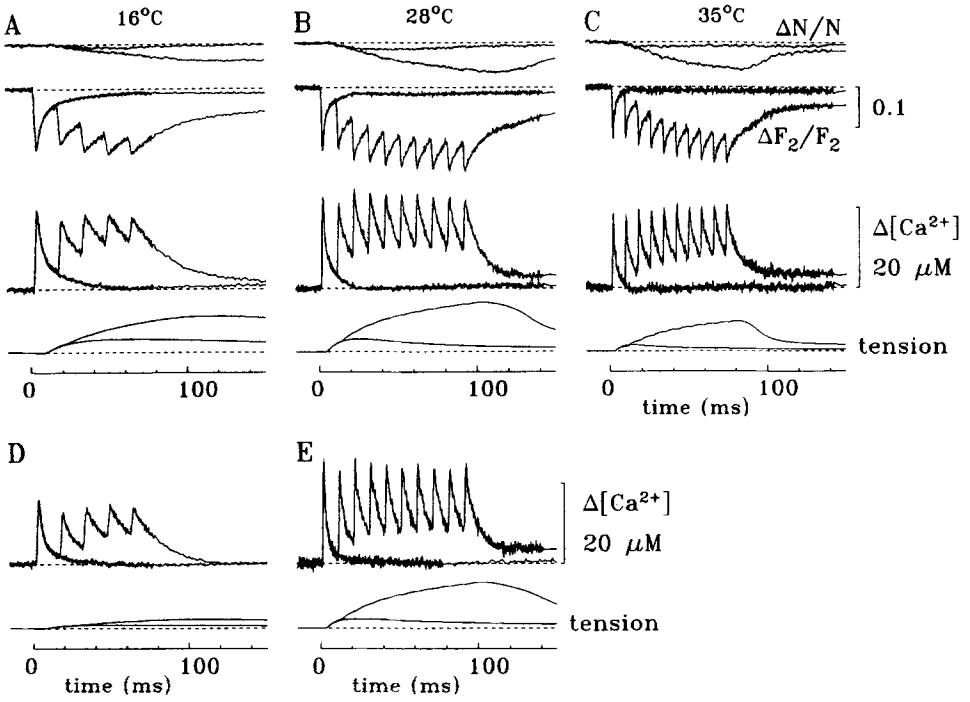

FIGURE 4. Examples of furaptra Ca^{2+} transients and tension in two fibers stimulated by high-frequency trains: *A*, *B*, and *C* at 16, 28, and 35°C, respectively (fiber 040896.1); *D* and *E* at 16 and 28°C, respectively (fiber 040996.3). All measurements used the ratio technique (illustrated in Fig. 1 *B*); examples of the ΔN/N and $\Delta F_2/F_2$ signals are shown for fiber 040896.1. The following values apply to fibers 040896.1 and 040996.3, respectively: time after injection, 19–77 and 17–42 min; indicator concentration, 62–117 and 85–113 μM; fiber diameter, 45 and 42 (assumed) μm; sarcomere length, 3.8 μm and not measured; number of stimuli per trace, 3–4 and 3.

Properties of $\Delta[Ca^{2+}]$ during High-frequency Stimulation

In five experiments, $\Delta[Ca^{2+}]$ and tension were measured at 16°C in response to a brief, high-frequency train of stimuli (e.g., 67 Hz for 75–150 ms); responses to trains were also measured in four experiments at 28°C (100 Hz for 100 ms) and in one experiment at 35°C (125 Hz for 80 ms). Fig. 4 shows examples of these responses, along with the single-twitch responses measured at the same time. The upper panels illustrate results from one experiment at three different temperatures (16, 28, and 35°C), whereas the lower panels show results from another experiment at two temperatures (16 and 28°C). In all panels, $\Delta[Ca^{2+}]$ and tension responses are shown. Additionally, the upper panels show the ΔN/N and $\Delta F_2/F_2$ traces that were used for calculation of the ratio $(\Delta F_2'/F_2)$ and Δf_{CaD} signals (not shown). The ΔN/N traces in this experiment indicate that movement of the fiber bundle during the tetani produced fractional decreases in the number of furaptra molecules within the recording field of peak amplitude −0.04 to −0.07. The ΔN/N waveforms are generally similar to the tension responses recorded at the end of the bundle (lowermost traces of panels *A–C*).

At 16°C (Fig. 4, *A* and *D*), the peak of $\Delta[Ca^{2+}]$ that resulted from the second shock was 15–20% smaller than that from the first shock, whereas, in response to the later shocks, the peak of $\Delta[Ca^{2+}]$ recovered towards the level produced by the first shock. Interestingly, the initial rate at which $\Delta[Ca^{2+}]$ declined from its peak value became progressively slower as a function of the shock number within the train. For example, in *A*, the initial decline of $\Delta[Ca^{2+}]$ after the first peak was characterized by a rate constant of 169 s^{-1} whereas for the second, third, and fifth peaks the rate constants were 70, 41, and 37 s^{-1}, respectively. In *D*, the corresponding rate constants were 250, 109, 61, and 56 s^{-1} (first, second, third, and fifth peaks, respectively). (Note:

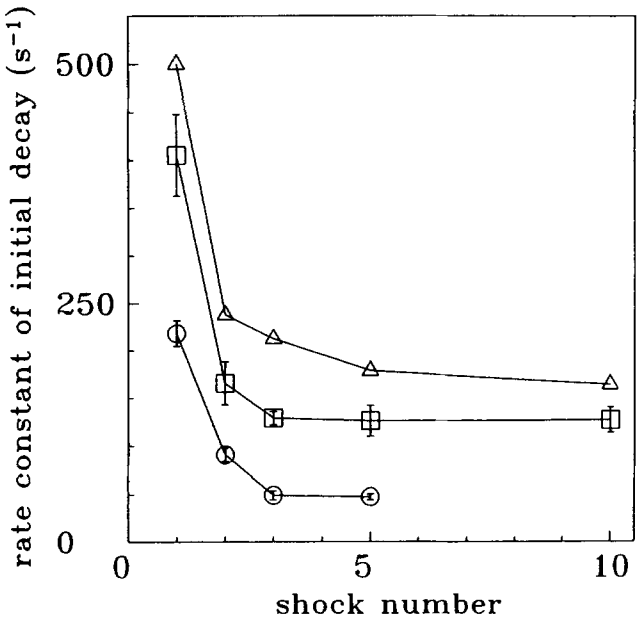

FIGURE 5. The ordinate plots the rate constants for the initial decay of $\Delta[Ca^{2+}]$ from the peaks observed during a train of stimuli, as estimated by the method given in the text. The abscissa gives the shock number during the train. Data are shown at three temperatures: *circles*, 16°C (n = 5); *squares*, 28°C (n = 4); *triangles*, 35°C (n = 1). The error bars extending from the 16 and 28°C data points give ±SEM.

to estimate these rates, a function for a single exponential decay to a final level of zero was fitted to the $\Delta[Ca^{2+}]$ traces beginning just after the time of the peak and extending for an interval of ~5 ms.)

Very similar results were seen in the three other multiple-shock experiments at 16°C. For the five experiments, the amplitude of the second peak of $\Delta[Ca^{2+}]$ compared to the first was 0.81 ± 0.03, and the average amplitude of the third through fifth peaks compared to the first was 0.88 ± 0.02. For the decay of $\Delta[Ca^{2+}]$ from peak, the average rate constants were 218 ± 13 s^{-1} for the first peak, 90 ± 7 s^{-1} for the second peak, 49 ± 5 s^{-1} for the third peak, and 48 ± 3 s^{-1} for the fifth peak.

Results at the higher temperatures, which used 10-shock trains, are illustrated in Fig. 4, *B*, *E*, (28°C) and *C* (35°C). Within any particular train, the $\Delta[Ca^{2+}]$ amplitudes of the second through tenth peaks were similar to that of the first peak, whereas the initial rate of decline of $\Delta[Ca^{2+}]$ from peak again slowed progressively during the train. At 28°C, the average values (n = 4) for the rates of decline from peak were 406 ± 43 s^{-1} (first peak), 166 ± 23 s^{-1} (second peak), 129 ± 7 s^{-1} (third peak), and 127 ± 13 s^{-1} (tenth peak). For the single experiment at 35°C, the rates of decline were 500 s^{-1} (first peak), 238 s^{-1} (second peak), 213 s^{-1} (third peak), and 151 s^{-1} (tenth peak).

After termination of the stimulus train, $\Delta[Ca^{2+}]$ in most of the panels of Fig. 4 appeared to return close to, but remain elevated above, baseline. Similar results were seen in the other multiple-shock experiments (not shown). However, the actual contribution of a maintained $\Delta[Ca^{2+}]$ signal to the baseline offset after a train is uncertain. First, as mentioned above, the ratio technique applied to bundles of fibers at the sarcomere lengths used in these experiments does not appear to completely eliminate all movement artifacts; moreover, the bundle movements were substantially larger during tetani than during single twitches (cf., the $\Delta N/N$ traces in Fig. 4, *A–C*). Second, furaptra is sensitive to Mg^{2+} as well as to Ca^{2+} (cf., MATERIALS AND METHODS), and there is likely to be a contribution of $\Delta[Mg^{2+}]$ to the baseline offset signal that may exceed the contribution of $\Delta[Ca^{2+}]$ (cf., the experiments of Konishi et al. [1991] in frog fibers, which estimated that about two-thirds of furaptra's offset signal is due to $\Delta[Mg^{2+}]$ and about one-third to $\Delta[Ca^{2+}]$). Because of the uncertainty in the mouse experiments concerning the contribution of movement artifacts to the baseline offset after a train, no attempt was made to estimate the combined contributions of $\Delta[Ca^{2+}]$ and $\Delta[Mg^{2+}]$ to the offset signal.

Fig. 5 presents a graphical summary of the initial rates of decline of $\Delta[Ca^{2+}]$ from peak during trains of the type illustrated in Fig. 4. With stimulation, rates decreased severalfold from the high value observed after the first shock to a nearly constant ("steady-state") value observed after a few shocks; more than half of the decrease in rate occurred between the first and second shocks. If rates were plotted as a function of time after onset of stimulation (not shown), the time required for the rate to decrease to half of the high rate was ~10 ms at 16°C (67 Hz stimulus), ~6 ms at 28°C (100 Hz stimulus), and ~5 ms at 35°C (125 Hz stimulus). The relative decrease in amplitude of the rate constant varied somewhat with temperature. At 16°C, the rate fell by a factor of 4.6 between the high and steady-state level; the corresponding factors for 28 and 35°C are 3.3 and 3.1, respectively.

After the last shock in a train, the full time course of $\Delta[Ca^{2+}]$'s return toward baseline could be followed and was always well described by a single exponential decay to a small baseline offset (not shown). The average rates estimated for this decay were 52 ± 3 s^{-1} at 16°C (n = 5), 146 ± 13 s^{-1} at 28°C (n = 4) and 152 s^{-1} at 35°C (n = 1). (Note: these values are slightly larger than the steady-state values shown in Fig. 5 (mentioned above) of 48 ± 3 s^{-1} at 16°C, 127 ± 13 s^{-1} at 28°C and 151 s^{-1} at 35°C. These latter values were based on fits to the initial decay and assumed no baseline offset, whereas, in the fits to the full time course of the decay, the value of the offset was usually a positive fraction of the last peak [0.086 ± 0.032; range, −0.045 to +0.259].)

Properties of $\Delta[Ca^{2+}]$ in Small-diameter Frog Fibers

As mentioned in the first section of RESULTS, the half-width of furaptra's Δf_{CaD} signal in mouse EDL fibers at 16°C (5.2 ± 0.4 ms; Table I) is only about half that measured previously in fast-twitch fibers of frog (10.9 ± 0.7 ms; Zhao et al., 1996). A similar difference also applies to the estimated half-width of $\Delta[Ca^{2+}]$ (4.6 ± 0.3 ms for mouse, row 1 of Table II; 9.6 ± 0.6 ms for frog, row 3 of Table II). One factor that might contribute to this difference in time courses is the diameter of the fibers; the average diameter in mouse fibers (40–45 μm, cf. Table I) is only about half that found in ordinary-sized frog fibers (80–90 μm). To investigate this possibility, we have measured $\Delta[Ca^{2+}]$ with furaptra in three frog single fibers of unusually small diameter: 45, 45, and 51 μm (measured at sarcomere lengths 3.5–3.8 μm). The other experimental conditions were as described in Zhao et al. (1996); the estimated myoplasmic furaptra concentrations were 0.04–0.21 mM. Row 4 of Table II summarizes the results. For these small-diameter frog fibers, the average half-width of $\Delta[Ca^{2+}]$ was 8.6 ± 1.6 ms (16°C). This value is very similar to that found for ordinary size frog fibers (9.6 ± 0.6 ms; row 3 of Table II) but is, again, about twice that found for mouse fibers. (The average amplitude of $\Delta[Ca^{2+}]$ is also similar for small and ordinary size frog fibers: 16.9 ± 1.5 μM and 16.5 ± 0.9 μM, respectively, rows 4 and 3 of Table II.) Thus, fiber-diameter differences appear to be ruled

out as an explanation for the faster time course of $\Delta[Ca^{2+}]$ in fast-twitch fibers of mouse.

DISCUSSION

$\Delta[Ca^{2+}]$ in intact EDL fibers of mouse was measured with furaptra and, in response to a single shock or brief high-frequency train of shocks, was resolved with a large signal-to-noise ratio. This resolution was achieved at relatively small myoplasmic concentrations of furaptra (0.04–0.13 mM); thus $\Delta[Ca^{2+}]$ is unlikely to have been altered significantly by the presence of the indicator (Konishi et al., 1991). Because furaptra is a rapidly responding indicator (Konishi et al., 1991; Zhao et al., 1996), we believe that our measurements supply the first accurate information about the rapid time course of $\Delta[Ca^{2+}]$ in intact, fast-twitch fibers of mammals. Moreover, based on previous studies in frog fibers that compared $\Delta[Ca^{2+}]$ measured with a number of lower-affinity indicators (Konishi et al., 1991; Zhao et al., 1996; see also Hirota et al., 1989), we believe that our furaptra measurements (calibrated as described in MATERIALS AND METHODS) supply the most accurate information to date about the amplitude of $\Delta[Ca^{2+}]$ in mammalian fibers. Although it is possible that the properties of $\Delta[Ca^{2+}]$ may have been altered by stretch of the fibers to long sarcomere lengths (>3.6 μm), such alterations are probably small; for example, in frog fibers, $\Delta[Ca^{2+}]$ is affected in only minor ways by changes in sarcomere length between 2.5 and 4.4 μm (Konishi et al., 1991).

During a twitch at 16°C, $\Delta[Ca^{2+}]$ was remarkably similar in the eight EDL fibers studied. Its time course was substantially briefer than that previously measured in intact frog fibers (semitendinosus or ilio-fibularis m.) under similar experimental conditions (Table II). For example, the half-width of $\Delta[Ca^{2+}]$ in mouse fibers, 4.6 ± 0.3 ms, is only about half that measured in frog fibers (9.6 ± 0.6 ms for ordinary-sized frog fibers; 8.6 ± 1.6 ms for small-diameter frog fibers).

In contrast, at 16°C the amplitude of Δf_{CaD} from furaptra was essentially the same for mouse and frog fibers: 0.153 ± 0.003 for mouse (Table I), 0.142 ± 0.008 for usual-sized frog fibers (Zhao et al., 1996), and 0.145 ± 0.013 for the small-diameter frog fibers. Under the reasonable assumption that furaptra's myoplasmic K_D is similar in mouse and frog myoplasm, it follows that the amplitude of $\Delta[Ca^{2+}]$ must be similar in mouse and frog, irrespective of the exact value of K_D (cf. Table II).

Comparisons with Other Measurements of $\Delta[Ca^{2+}]$ in Mammalian Fibers during Twitch and Tetanus

Intact rat fibers. The first Ca^{2+} measurements in mammalian muscle compared the time course of aequorin light signals in fast-twitch (EDL) and slow-twitch (soleus) fibers of rat muscle (Eusebi et al., 1980, 1985). A faster decay of the aequorin signal in EDL than in soleus fibers (mean decay rate constants of 63 and 24 s^{-1}, respectively, after a 20–25-ms voltage-clamp pulse; Eusebi et al., 1980, 1985) gave the first indication that $\Delta[Ca^{2+}]$ time courses probably differ significantly in different fiber types (see also Carroll et al., 1995*b*; Rome et al., 1995, 1996). On the other hand, because aequorin responds to $\Delta[Ca^{2+}]$ with a substantial delay (see, e.g., Blinks et al., 1978), it is not surprising that the time to peak of the aequorin signal in EDL fibers (10 ms after the peak of the action potential, 25°C; Eusebi et al., 1985) is markedly slower than that which we measure with furaptra (2 ms after a brief external shock, 28°C; Table II).

Intact mouse FDB fibers. Most subsequent studies of $\Delta[Ca^{2+}]$ in mammalian fibers have used fluorescent indicators. In the studies on single, intact FDB fibers of mouse, indo-1 (and occasionally fura-2) was used and fibers were activated primarily by tetanic stimulation (Westerblad et al., 1993; Westerblad and Allen, 1993*a*, 1993*b*, 1994, 1996). Because high-affinity indicators like indo-1 and fura-2 respond to $\Delta[Ca^{2+}]$ in skeletal muscle with substantial delays, signals from these indicators cannot give temporally accurate information about rapid changes in $[Ca^{2+}]$ unless substantial kinetic corrections are applied to the measurements (Baylor and Hollingworth, 1988; Klein et al., 1988; Carroll et al., 1995*a*; Zhao et al., 1996). For example, without correction for the slow kinetics of indo-1, the half-width of $\Delta[Ca^{2+}]$ during a twitch of FDB fibers at 22°C appears to be ~13 ms (Fig. 1 of Westerblad and Allen, 1994; sarcomere spacing, ~2.4 μm); this value is markedly slower than the 3.3 ms value estimated by linear interpolation of our furaptra data at 16 and 28°C (rows 1 and 2 of Table II). During sustained stimulation, $\Delta[Ca^{2+}]$ changes more slowly and estimation of temporal properties will be less affected by the slow kinetics of indo-1. Nevertheless, kinetic limitations may affect indo-1 signals during many types of sustained stimulation. For example, the indo-1 data of Westerblad and Allen (Table 1 of 1993*b*; Fig. 4 of 1994) imply a rate constant of ~27 s^{-1} at 22°C for the early decline of $\Delta[Ca^{2+}]$ after a 100-ms tetanus (70–100 Hz, under "control" conditions). In contrast, our furaptra data imply a decay rate of ~88 s^{-1} after a similar stimulus (based on a linear interpolation between the decay rates given in RESULTS, 48 s^{-1} at 16° and 127 s^{-1} at 28°C; see also Fig. 5). Although experimental conditions are not exactly comparable for their FDB and our EDL fibers, a difference this large suggests that indo-1 does not accurately monitor the most rapid changes in $[Ca^{2+}]$ during such tetanic stimulations.

In FDB fibers, the peak amplitude of $\Delta[Ca^{2+}]$ cali-

brated from indo-1 is surprisingly small, in the range 0.5–1.0 μM for a brief, 70 Hz tetanus (Westerblad and Allen, 1993*a*, 1994, 1996). Since indo-1 does not respond rapidly to changes in $[Ca^{2+}]$, our furaptra data obtained during high-frequency stimulation should be time-averaged for comparison with the data of Westerblad and Allen. From data such as those shown in Fig. 4, we estimate that, during a 70–100 Hz, 100 ms tetanus of EDL fibers, the time-averaged value of $\Delta[Ca^{2+}]$ at 22°C is 11–12 μM; this value is 11–24-fold larger than that reported for FDB fibers. A small part of this difference is explained by the values assumed for the K_D's of the indicators in the myoplasmic environment. The value assumed for indo-1 (0.18 μM; Westerblad and Allen, 1993*b*) is essentially identical to that measured in a simple salt solution (0.21 μM), whereas the value we assume for furaptra (93 μM at 22°C) is about twofold larger than applicable to a simple salt solution (see MATERIALS AND METHODS and cited references concerning the likelihood that indicator K_D's are elevated by the myoplasmic environment). Under the assumption that the K_D's of indo-1 and furaptra are either unaltered or similarly altered by the myoplasmic environment, there is still a large (6–12-fold) difference in the amplitude of $\Delta[Ca^{2+}]$ calibrated with indo-1 and furaptra. Although some of this difference might be related to the use of different muscles (FDB vs. EDL), two other possibilities, which relate to the properties of the indicators, appear to be more likely. (*a*) Because the percentage of indicator molecules that are bound to myoplasmic constituents is larger for indo-1 than for furaptra, at least in frog fibers (81 ± 5% vs. 58 ± 2%; Zhao et al., 1996), the factor by which K_D is elevated by the myoplasmic environment is likely to be larger for indo-1 than for furaptra. (*b*) As pointed out by Hirota et al. (1989) (see also Westerblad and Allen, 1996), $\Delta[Ca^{2+}]$ signals measured with high-affinity indicators that approach saturation during activity are susceptible to some types of potentially large calibration errors that are avoided by lower-affinity indicators that function close to their linear range.

Cut rat EDL fibers. Delbono and Stefani (1993), the first authors to use furaptra in mammalian fibers, studied cut fiber segments of rat EDL mounted in a vaseline-gap apparatus. In response to a single action potential, the values reported for time to peak and half-width of $\Delta[Ca^{2+}]$ were 4.6 ± 0.4 ms and 8.2 ± 1.5 ms, respectively (17°C; sarcomere lengths, 3.6–3.8 μm). Their value for time to peak is essentially identical to that measured by us in mouse EDL fibers at 16°C (4.4 ± 0.2 ms; col. 4 of Table II); in contrast, their value for the half-width of $\Delta[Ca^{2+}]$ is significantly larger than ours (4.6 ± 0.3 ms; col. 5 of Table II). We do not know if this latter difference reflects a physiological difference in $\Delta[Ca^{2+}]$ in rat vs. mouse fibers or is a consequence of some experimental difference, e.g., the use of cut vs. intact fibers.

There also appears to be a substantial difference between cut rat EDL fibers and intact mouse EDL fibers regarding the peak amplitude of $\Delta[Ca^{2+}]$ during a twitch: 4.6 ± 0.4 μM (Delbono and Stefani, 1993) vs. 17.8 ± 0.4 μM (col. 7 of Table II). However, there is some uncertainty in the $\Delta[Ca^{2+}]$ calibration of Delbono and Stefani (1993) because the peak values of Δf_{CaD} and $\Delta[Ca^{2+}]$ given in their Fig. 3 *A* (0.043 and 4.3 μM, respectively) are not consistent with the 49 μM value assumed for K_D. Moreover, Delbono and Stefani (1993) did not report raw values of $\Delta F/F$ in their action potential experiments; thus a direct comparison of their data with ours is not possible.

Enzymatically dissociated rat FDB fibers. Carroll et al. (1995*a*) estimated properties of $\Delta[Ca^{2+}]$ in single enzymatically dissociated fibers of rat FDB muscle at a sarcomere length of ~1.9 μm. The fibers were AM-loaded with fura-2 at 37°C, and ratio fluorescence measurements were made at 28-30°C. Importantly, before estimation of $\Delta[Ca^{2+}]$ properties, the ratio measurements were corrected for fura-2's slow intracellular reaction rates with Ca^{2+} (Baylor and Hollingworth, 1988; Klein et al., 1988; also see above). The correction for fura-2's kinetic delay was checked against AM-loaded furaptra measurements from other fibers and judged to be adequate. The time course of $\Delta[Ca^{2+}]$ so determined in rat FDB fibers had some similarities as well as some substantial differences in comparison with time courses measured by us for mouse EDL fibers at 28°C. In response to a single shock, the half-width of $\Delta[Ca^{2+}]$ in rat fibers was 9–10 ms (Fig. 4 of Carroll et al., 1995*a*), a value 4–5 times that which we report for mouse (2.0 ± 0.1 ms; col. 6 of Table II). At later times after a single shock, the return of $\Delta[Ca^{2+}]$ to baseline had a prominent slow phase in rat fibers, which often lasted 50 ms or longer (Figs. 2-5 of Carroll et al., 1995a); in our mouse measurements, a similar slow phase was not detected (cf. Fig. 2, *E* and *F*). In response to 100 Hz trains of stimuli, individual peaks of $\Delta[Ca^{2+}]$ were well-resolved in both rat (Figs. 5 and 6 of Carroll et al., 1995*a*) and mouse (our Fig. 4). In some rat fibers, the later peaks of $\Delta[Ca^{2+}]$ were smaller than or comparable to that of the first peak (as in our Fig. 4) whereas, in other rat fibers, the amplitudes of later peaks rose to successively higher levels (in contrast to our results; cf. Fig. 4).

The peak amplitude of $\Delta[Ca^{2+}]$ in these rat fibers was 0.2–1 μM for a single twitch and 0.2–2 μM for a brief, 100 Hz tetanus (Figs. 2–7 of Carroll et al., 1995*a*). These values are 10–100-fold smaller than the ~20 μM values that we report at 28°C (col. 7 of Table II and Fig. 4, *B* and *E*). A significant part (~10-fold) of this discrepancy is attributable to the selection of fura-2's intracellular K_D. Carroll et al. (1995*a*) used a K_D of 0.05–

0.07 μM, whereas our previous measurements with fura-2 and furaptra in frog fibers are consistent with a 10-fold larger value for fura-2 (0.69 μM; Hollingworth et al., 1992). The remaining discrepancy in amplitudes, which is as large as 10-fold for some comparisons, suggests that the peak of $\Delta[Ca^{2+}]$ in enzymatically dissociated rat FDB fibers at short sarcomere length is smaller, and more variable, than that of intact mouse EDL fibers at long sarcomere length.

Effects of Temperature on $\Delta[Ca^{2+}]$ and Tension Responses during Twitch and Tetanus

As described in RESULTS, $\Delta[Ca^{2+}]$ and tension responses were measured at different temperatures, both during single twitches (Figs. 2 and 4) and in response to brief trains of stimuli (Fig. 4). Temperature affected our tension recordings in a manner that was generally consistent with the more complete study of Lannergren and Westerblad (1987), which was carried out on singly dissected FDB fibers at physiological sarcomere lengths. In that study, and in ours, (*a*) twitch tension at temperatures below 10°C was a small fraction of that observed at 15–30°C, (*b*) tetanic tension increased markedly as temperature was increased between 10 and 30°C, and (*c*) tetanic tension decreased as temperature was raised above 30°C, in some cases irreversibly.

Regarding $\Delta[Ca^{2+}]$, our results indicate that the peak amplitude of $\Delta[Ca^{2+}]$ during a twitch changed in parallel with the change in twitch amplitude — decreasing substantially with cooling below 16°C and increasing somewhat with warming above 16°C (Figs. 2 and 3 *A*). The half-width of $\Delta[Ca^{2+}]$ during a twitch also changed markedly with temperature, falling by about a factor of 10 between 5 and 35°C (Fig. 3 *B*). As temperature was increased between 16 and 35°C there was a substantial speeding of the rate of decline of $\Delta[Ca^{2+}]$ after a twitch or brief high-frequency train of stimuli (Fig. 5). The Q_{10} for this effect is approximately 2 (not shown), a value consistent with the Q_{10} of 2.3 reported for the decay of the aequorin signal in rat EDL fibers stimulated by a 20–25-ms voltage-clamp depolarization (15-40°C; Eusebi et al., 1985).

Ca^{2+} Binding to Troponin Estimated from $\Delta[Ca^{2+}]$ during a Tetanus

Because the amplitude that we estimate for $\Delta[Ca^{2+}]$ in mammalian fast-twitch fibers is 4–100-fold larger than that reported by other laboratories, it is important to consider how these amplitudes relate to expected levels of thin filament activation and force production. To address this question, we have applied computer modeling to our $\Delta[Ca^{2+}]$ measurements at 28°C to estimate the fractional occupancy of the Ca^{2+}-regulatory sites on troponin. These calculations were carried out under the assumption that $K_{D,Ca}$, the apparent dissociation constant of the regulatory sites for Ca^{2+}, is 1.3 μM, i.e., the same as measured for troponin on reconstituted thin filaments of rabbit skeletal muscle (free $[Mg^{2+}]$ = 1 mM, temperature = 25°C; Zot and Potter, 1987). These calculations are identical in principle to the mass-action calculations described previously for frog fibers at 16°C (Baylor et al., 1983; Baylor and Hollingworth, 1988; cf. Robertson, Johnson and Potter, 1981). For the present calculations, the rate constants of the Ca^{2+}-troponin reaction were increased twofold to reflect the higher temperature of the $\Delta[Ca^{2+}]$ measurements (28 vs. 16°C); the values assumed were $1.77 \times 10^8\ M^{-1}\ s^{-1}$ for k_{+1} (the association rate constant) and $230\ s^{-1}$ for k_{-1} (the dissociation rate constant).

In Fig. 6, the lowermost trace shows the tension transient, the next trace the $\Delta[Ca^{2+}]$ signal estimated with furaptra, and the next trace (continuous trace, *f*) the computed probability that a Ca^{2+}-regulatory site on troponin is occupied by Ca^{2+}. Additionally, since there appear to be two identical and independent regulatory

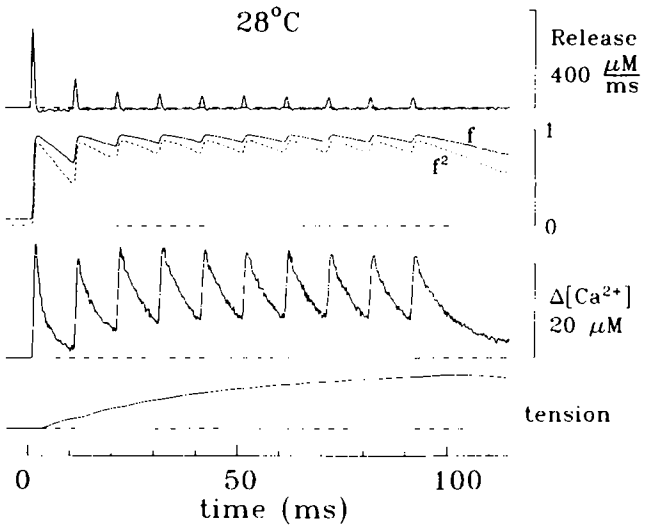

FIGURE 6. Computer modeling based on an average $\Delta[Ca^{2+}]$ signal measured in response to a 100-ms, 100-Hz stimulus from three mouse fibers at 28°C. The tension and $\Delta[Ca^{2+}]$ traces were averaged from fibers 032596.2, 040896.1, and 040996.3 (the experiments for which the data sampling periods were identical). To reduce baseline noise in the modeled traces, the $\Delta[Ca^{2+}]$ signal was set to zero before rise of the signal. The trace labeled *f* (continuous) is the estimated fractional occupancy by Ca^{2+} of troponin's Ca^{2+}-regulatory sites; its square is labeled f^2 (dashed line). Occupancy was computed from the Ca^{2+} transient (see text), with k_{+1} and k_{-1} values of $1.77 \times 10^8\ M^{-1}\ s^{-1}$ and $230\ s^{-1}$, respectively, assumed for the Ca^{2+}-troponin reaction (28°C; $K_{D,Ca}$ = 1.3 μM). Resting $[Ca^{2+}]$ was set to 0.1 μM. The uppermost trace represents a lower limit for the rate at which Ca^{2+} is released from the SR into the myoplasm during the stimulation period. Negative excursions in this trace reflect a net movement of the released Ca^{2+} onto the Ca^{2+} removal systems (parvalbumin and the SR Ca^{2+} pump).

sites on each troponin molecule (Zot and Potter, 1987), this panel also shows the square of this probability (dashed trace, f^2). The f^2 trace thus estimates the probability of simultaneous occupancy of the two regulatory sites on any particular troponin molecule and is presumed to be closely related to the extent and time course of thin-filament activation.

In Fig. 6, the $\Delta[Ca^{2+}]$ transients became essentially constant during the last 80% of the stimulation period, with the peaks of $\Delta[Ca^{2+}]$ reaching ~22 μM; during the same period, the time-averaged value of $\Delta[Ca^{2+}]$ was 13.8 μM. The corresponding peak and time-averaged values for f are 0.94 and 0.91, respectively, whereas those for f^2 are 0.88 and 0.83, respectively. The estimation that f and f^2 rise to levels that approach 1.0 seems reasonable, given that the tetanic tension measured in intact fibers at a normal sarcomere spacing (~390 kNewtons/m^2, 25°C; Lannergren and Westerblad, 1987) is similar to the saturating level of tension observed in skinned fibers in tension-pCa measurements (~400 kNewtons/m^2, 35°C; Stephenson and Williams, 1981). Thus the traces in Fig. 6 indicate that there is reasonable agreement between the calibration of our furaptra $\Delta[Ca^{2+}]$ signal and the 1.3 μM value reported for $K_{D,Ca}$ of the Ca^{2+}-regulatory sites on reconstituted thin filaments (Zot and Potter, 1987).

Given this conclusion, it is of interest to consider the implications of a much smaller calibrated amplitude for time-averaged $\Delta[Ca^{2+}]$ during a tetanus, e.g., the ~0.5–1 μM value estimated from indo-1 by Westerblad and Allen (1993*a*, 1993*b*, 1994, 1996) or the 0.2–2 μM value estimated from fura-2 by Carroll et al. (1995*a*). According to the experiments of Westerblad and Allen (1993*b*), which used variable stimulation frequencies to alter the amplitude of tension and time-averaged $\Delta[Ca^{2+}]$ during a tetanus, the value of $[Ca^{2+}]$ that activates 50% of maximum tension (Ca_{50}) is 0.36 μM. If Ca_{50} corresponds to f and f^2 values of 0.7 and 0.5, respectively, as indicated by the data of Zot and Potter (1987; Fig. 3 *B*) and Zot et al. (1986; Fig. 2), the implied value of $K_{D,Ca}$ is 0.15 μM. This value is eight- to ninefold smaller than the 1.3 μM value reported by Zot and Potter (1987) and likely implies an eight- to ninefold decrease in k_{-1} in comparison with the value used in our Ca^{2+}-troponin calculations (Fig. 6). (Note: estimates of k_{+1} for isolated troponin C molecules are large, 1–2 × 10^8 M^{-1} s^{-1} [4°C; Johnson et al., 1994]. The possibility of a substantial increase in k_{+1} in myoplasm at 22–28°C may be considered unlikely, since any increase in k_{+1} due to the higher temperature would likely be counter-balanced by a decrease due to the higher viscosity of myoplasm, which is about twice that of a simple salt solution [Kushmerick and Podolsky, 1969].)

An eight- to ninefold reduction in k_{-1} implies a value no larger than ~30 s^{-1} (= 0.15 × 10^{-6} M · 2 × 10^8 M^{-1} s^{-1}). Although values of k_{-1} are difficult to measure in vivo, some new information about k_{-1} values has recently been obtained from experiments on superfast fibers of toadfish swimbladder (Rome et al., 1996). Under the assumption that the extremely rapid relaxation of tension observed in superfast fibers must be preceded by the dissociation of Ca^{2+} from troponin, the implied value of k_{-1} in this fiber type is at least 350 s^{-1} at 16°C, or perhaps 400 s^{-1} at 22°C. Furthermore, as argued by Rome et al. (1996), the relative positioning of the tension-pCa curves of different fiber types suggests that the value of k_{-1} for ordinary fast-twitch fibers of toadfish or frog is about one-third the value of swimbladder fibers, and a similar factor would also apply to fast-twitch fibers of mammal. This suggests that k_{-1} for mammalian fibers at 22°C is at least 135 s^{-1} (400/3) and that the much smaller value implied by the 1 μM calibration for tetanic $\Delta[Ca^{2+}]$ is improbable.

A Possible Explanation for the Progressive Slowing of the Initial Rate of Decay of $\Delta[Ca^{2+}]$ during a Tetanus

As noted in RESULTS, when a fiber was activated by a high-frequency train of stimuli, the initial decay of $\Delta[Ca^{2+}]$ from its individual peaks slowed progressively during the train. Most of this decrease in rate occurred between the first and second shocks of the train (Fig. 5). An effect of this sort would be expected if one or more of the high-capacity Ca^{2+} binding proteins of myoplasm rapidly bound Ca^{2+} to a near maximal level relatively early during a train of Ca^{2+} release events. Possible binding sites of this sort include the Ca^{2+}-regulatory sites on troponin, the metal-free sites on parvalbumin, and the Ca^{2+} transport sites on the SR Ca^{2+} pump. With regard to the first possibility, it is of interest to note how the transient increments in trace f of Fig. 6 change with shock number. If Δf_N denotes the increment in f due to the Nth shock, Δf_1, at 0.86, is by far the largest such increment; Δf_2 is only about one-third of Δf_1, and subsequent Δf_N's are only about 1/10th of Δf_1. Thus there is a close parallel between the progressive decrease in amplitude of Δf_N and the decrease in the initial rate of decay of $\Delta[Ca^{2+}]$ (Fig. 5). This rate decrease is thus consistent with the idea that one (or more) of the high-capacity Ca^{2+}-binding sites of myoplasm achieves a near steady-state occupancy with Ca^{2+} quite early during a high-frequency tetanus and is thereafter unavailable to assist in the lowering of $\Delta[Ca^{2+}]$. In this regard, it will be of interest in future experiments to measure, after cessation of stimulation, the time course that describes the recovery of the $\Delta[Ca^{2+}]$ decay rate to its initial level. This recovery time course will presumably reflect the rate of dissociation of Ca^{2+} from its putative myoplasmic binding site(s).

A Lower Limit for the Rate of SR Ca^{2+} Release in Mammalian Fibers

Given $\Delta[Ca^{2+}]$ recorded with a rapidly-responding Ca^{2+} indicator, it is of interest to use the computational model of Baylor et al. (1983; "model 2," developed for use in frog fibers) to estimate the rate at which Ca^{2+} is released from the sarcoplasmic reticulum (SR) into the myoplasm in response to electrical stimulation. The upper trace in Fig. 6 shows an example of this model applied to mouse fibers. For this calculation, the increase in total Ca^{2+} concentration in the myoplasmic water volume ($\Delta[Ca_T]$, not shown) was estimated as the sum of the increases in three myoplasmic pools: the free pool ($\Delta[Ca^{2+}]$ trace in Fig. 6), the Ca^{2+} bound to furaptra (not shown; peak value of 10 μM) and the Ca^{2+} bound to the Ca^{2+}-regulatory sites on troponin. The latter increase was estimated from the f trace shown in Fig. 6 after multiplication by the factor 240 μM (the concentration of the Ca^{2+}-regulatory sites if referred to the myoplasmic water volume; Baylor et al., 1983). Our estimate of $\Delta[Ca_T]$ is, in fact, a lower limit, since some released Ca^{2+} must also rapidly bind to myoplasmic sites on parvalbumin and the SR Ca^{2+} pump. The uppermost trace in Fig. 6, which is the time derivative of $\Delta[Ca_T]$, thus provides a lower limit for the SR Ca^{2+} release rate. In response to the first shock, the peak of the release trace was 327 μM/ms (28°C); subsequent peaks were substantially smaller (122 μM/ms for the second peak and 48 μM/ms for the fifth peak).

Similar estimations of the SR release rate (not shown) were carried out for trains of stimuli at 16 and 35°C (cf. the $\Delta[Ca^{2+}]$ signals shown in Fig. 4). To adjust for the temperature differences, the association and dissociation rate constants used for the Ca^{2+}-troponin reaction at 28°C were either divided by 2 (for the 16°C estimations) or multiplied by 2 (for the 35°C estimations). For the five experiments at 16°C, the average peak releases due to the first, second and fifth shocks were 151 ± 3, 39 ± 2, and 13 ± 2 μM/ms, respectively (67 Hz train). For the single experiment at 35°C, the corresponding peak values were 364, 167, and 71 μM/ms, respectively (125 Hz train).

These calculations of SR Ca release illustrate two main points. First, the rate of SR Ca^{2+} release decreases substantially during a high-frequency train of action potentials. This finding is similar to that reported for frog fibers (e.g., Baylor et al., 1983; Maylie et al., 1987; Baylor and Hollingworth, 1988) and, by analogy with frog, is presumed to occur mainly through an inactivation of the SR Ca^{2+} release channels that results from the associated rise in myoplasmic free $[Ca^{2+}]$ ("Ca^{2+}-inactivation of Ca^{2+} release") (Baylor et al., 1983; Schneider and Simon, 1988; Simon et al., 1991). The presence of Ca-inactivation of Ca release in mammalian fibers has previously been inferred from voltage-clamp experiments on cut rat fibers (Garcia and Schneider, 1993), and our experiments suggest that this inactivating effect of Ca^{2+} is likely to be strong.

Second, in response to a single action potential, the SR Ca^{2+}-release rate in fast-twitch mouse fibers is both large and brief. Indeed, at 16°C, the average peak rate that we estimate, 151 ± 3 μM/ms, is slightly larger than that which was estimated recently for fast-twitch fibers of frog, 142 ± 5 μM/ms (which, in contrast to the mouse calculations described here, included a small contribution for Ca^{2+} binding to parvalbumin; Hollingworth and Baylor, 1996). Moreover, the half-width of the release event is significantly briefer in mouse than in frog (1.5 ± 0.0 vs. 2.2 ± 0.1 ms, respectively). Our finding of a close similarity between the amplitude of Ca^{2+} release events in mouse and frog contrasts with a recent report based on voltage-clamp experiments in cut fibers (Shirokova et al., 1996); in those experiments, the peak release rate reported for depolarizations to ~0 mV was four- to fivefold larger in frog than rat fibers (31 ± 4 vs. 7 ± 2 μM/ms; 14°C). The reason for these quite different observations from cut fibers is not known, but our results suggest that conclusions about fundamental differences in control mechanisms between mammalian and amphibian muscle (Shirokova et al., 1996) should be viewed with caution.

We thank Dr. Knox Chandler for helpful comments on the manuscript.

This work was supported by grants to S.M. Baylor from the U.S. National Institutes of Health (NS 17620) and the Muscular Dystrophy Association.

Original version received 24 June 1996 and accepted version received 2 August 1996.

REFERENCES

Baker, A.J., R. Brandes, J.H.M. Schreur, S.A. Camacho, and M.W. Wiener. 1994. Protein and acidosis alter calcium-binding and fluorescence spectra of the calcium indicator indo-1. *Biophys. J.* 67: 1646–1654.

Baylor, S.M., W.K. Chandler, and M.W. Marshall. 1983. Sarcoplasmic reticulum calcium release in intact frog skeletal muscle fibres estimated from Arsenazo III calcium transients. *J. Physiol. (Lond.).* 344:625–666.

Baylor, S.M., and S. Hollingworth. 1988. Fura-2 calcium transients in frog skeletal muscle fibres. *J. Physiol. (Lond.).* 403:151–192.

Baylor, S.M., and H. Oetliker. 1977. A large birefringence signal preceding contraction in single twitch fibres of the frog. *J. Physiol. (Lond.).* 264:141–162.

Blinks, J.R., R. Rudel, and S.R. Taylor. 1978. Calcium transients in

isolated amphibian skeletal muscle fibres: detection with aequorin. *J. Physiol. (Lond.).* 277:291–323.

Carroll, S.L., M.G. Klein, and M.F. Schneider. 1995*a*. Calcium transients in intact rat skeletal muscle fibers in agarose gel. *Am. J. Physiol.* 269:C28–C34.

Carroll, S.L., M.G. Klein, and M.F. Schneider. 1995*b*. Calcium transients in rat intact fast- and slow-twitch skeletal muscle fibers. *Biophys. J.* 68:A177.

Delbono, O., and E. Stefani. 1993. Calcium transients in single mammalian skeletal muscle fibres. *J. Physiol. (Lond.).* 463:689–707.

Eusebi, F., R. Miledi, and T. Takahashi. 1980. Calcium transients in mammalian muscles. *Nature (Lond.).* 284:560–561.

Eusebi, F., R. Miledi, and T. Takahashi. 1985. Aeqorin-calcium transients in mammalian fast and slow muscle fibers. *Biochem. Research.* 6:129–138.

Garcia, J., and M.F. Schneider. 1993. Calcium transients and calcium release in rat fast-twitch skeletal muscle fibres. *J. Physiol. (Lond.).* 463:709–728.

Godt, R.E., and T.M. Nosek. 1989. Changes of intracellular milieu with fatigue or hypoxia depress contraction of skinned rabbit skeletal and cardiac muscle. *J. Physiol. (Lond.).* 412:155–180.

Goldman, Y.E., J. McCray, and K.W. Ranatunga. 1987. Transient tension changes initiated by laser temperature jumps in rabbit psoas muscle fibres. *J. Physiol. (Lond.).* 392:71–95.

Grynkiewicz, G., M. Poenie, and R.Y. Tsien. 1985. A new generation of Ca^{2+} indicators with greatly improved fluorescence properties. *J. Biol. Chem.* 260:3440–3450.

Hirota, A., W.K. Chandler, P.L. Southwick, and A.S. Waggoner. 1989. Calcium signals recorded from two new purpurate indicators inside frog cut twitch fibers. *J. Gen. Physiol.* 94:597–631.

Hollingworth, S., and S.M. Baylor. 1996. Sarcoplasmic reticulum (SR) calcium release in intact superfast toadfish swimbladder (tsb) and fast frog twitch muscle fibers. *Biophys. J.* 70:A235.

Hollingworth, S., A.B. Harkins, N. Kurebayashi, M. Konishi, and S.M. Baylor. 1992. Excitation-contraction coupling in intact frog skeletal muscle fibers injected with mmolar concentrations of fura-2. *Biophys. J.* 63:224–234.

Hove-Madsen, L., and D.M. Bers. 1992. Indo-1 binding to protein in permeabilized ventricular myocytes alters its spectral and Ca binding properties. *Biophys. J.* 63:89–97.

Johnson, J.D., R.J. Nakkula, C. Vasulka, and L.B. Smillie. 1994. Modulation of Ca^{2+} exchange with the Ca^{2+}-specific regulatory sites of troponin C. *J. Biol. Chem.* 269:8919–8923.

Klein, M.G., B.J. Simon, G. Szucs, and M.F. Schneider. 1988. Simultaneous recording of calcium transients in skeletal muscle using high- and low-affinity calcium indicators. *Biophys. J.* 53:971–988.

Konishi, M., and S.M. Baylor. 1991. Myoplasmic calcium transients monitored with purpurate indicator dyes injected in intact frog skeletal muscle fibers. *J. Gen. Physiol.* 97:245–270.

Konishi, M., S. Hollingworth, A.B. Harkins, and S.M. Baylor. 1991. Myoplasmic calcium transients in intact frog skeletal muscle fibers monitored with the fluorescent indicator furaptra. *J. Gen. Physiol.* 97:271–301.

Konishi, M., A. Olson, S. Hollingworth, and S.M. Baylor. 1988. Myoplasmic binding of fura-2 investigated by steady-state fluorescence and absorbance measurements. *Biophys. J.* 54:1089–1104.

Konishi, M., N. Suda, and S. Kurihara. 1993. Fluorescence signals from the Mg^{2+}/Ca^{2+} indicator furaptra in frog skeletal muscle fibers. *Biophys. J.* 64:223–239.

Kurebayashi, N., A.B. Harkins, and S.M. Baylor. 1993. Use of fura red as an intracellular calcium indicator in frog skeletal muscle fibers. *Biophys. J.* 64:1934–1960.

Kushmerick, M.J., and R.J. Podolsky. 1969. Ionic mobility in muscle cells. *Science (Wash. DC).* 166:1297–1298.

Lannergren, J., and H. Westerblad. 1987. The temperature dependence of isometric contractions of single, intact fibres dissected from a mouse foot muscle. *J. Physiol. (Lond.).* 390:285–293.

Maughan, D.W., J.E. Molloy, M.A.P. Brotto, and R.E. Godt. 1995. Approximating the isometric force-calcium relation of intact frog muscle using skinned fibers. *Biophys. J.* 69:1484–1490.

Maylie, J., M. Irving, N.L. Sizto, and W.K. Chandler. 1987. Calcium signals recorded from cut frog twitch fibers containing antipyrylazo III. *J. Gen. Physiol.* 89:83–143.

Metzger, J.M., and R.L. Moss. 1990. pH modulation of the kinetics of a Ca^{2+}-sensitive cross-bridge state transition in mammalian single skeletal muscle fibres. *J. Physiol. (Lond.).* 428:751–764.

Raju, B., E. Murphy, L.A. Levy, R.D. Hall, and R.E. London. 1989. A fluorescent indicator for measuring cytosolic free magnesium. *Am. J. Physiol.* 256:C540–C548.

Robertson, S.P., J.D. Johnson, and J.D. Potter. 1981. The time-course of Ca exchange with calmodulin, troponin, parvalbumin, and myosin in response to transient increases in Ca^{2+}. *Biophys. J.* 34:559–569.

Rome, L.C., D.A. Syme, S. Hollingworth, S.L. Lindstedt, and S.M. Baylor. 1995. The whistle and the rattle: the design of sound producing muscles. *Biophys. J.* 68:A17.

Rome, L.C., D.A. Syme, S. Hollingworth, S.L. Lindstedt, and S.M. Baylor. 1996. The whistle and the rattle: the design of sound producing muscles. *Proc. Natl. Acad. Sci. USA.* 93:8095–8100.

Schneider, M.F., and B.J. Simon. 1988. Inactivation of calcium release from the sarcoplasmic reticulum in frog skeletal muscle. *J. Physiol. (Lond.).* 405:727–745.

Shirokova, N., J. Garcia, G. Pizarro, and E. Rios. 1996. Ca^{2+} release from the sarcoplasmic reticulum compared in amphibian and mammalian skeletal muscle. *J. Gen. Physiol.* 107:1–18.

Simon, B.J., M.G. Klein, and M.F. Schneider. 1991. Calcium dependence of inactivation of calcium release from the sarcoplasmic reticulum in skeletal muscle fibers. *J. Gen. Physiol.* 97:437–471.

Stephenson, D.G., and D.A. Williams. 1981. Calcium-activated force responses in fast- and slow-twitch skinned muscle fibres of the rat at different temperatures. *J. Physiol. (Lond.).* 317:281–302.

Westerblad, H., and D.G. Allen. 1991. Changes of myoplasmic calcium concentrations during fatigue in single mouse muscle fibers. *J. Gen. Physiol.* 98:615–635.

Westerblad, H., and D.G. Allen. 1993*a*. The contribution of $[Ca^{2+}]_i$ to the slowing of relaxation in fatigued single fibres from mouse skeletal muscle. *J. Physiol. (Lond.).* 468:729–740.

Westerblad, H., and D.G. Allen. 1993*b*. The influence of intracellular pH on contraction, relaxation and $[Ca^{2+}]_i$ in intact single fibres from mouse muscle. *J. Physiol. (Lond.).* 466:611–628.

Westerblad, H., and D.G. Allen. 1994. Relaxation, $[Ca^{2+}]_i$ and $[Mg^{2+}]_i$ during prolonged tetanic stimulation of intact, single fibres from mouse skeletal muscle. *J. Physiol. (Lond.).* 480:31–43.

Westerblad, H., and D.G. Allen. 1996. Slowing of relaxation and $[Ca^{2+}]_i$ during prolonged tetanic stimulation of single fibres from *Xenopus* skeletal muscle. *J. Physiol. (Lond.).* 492:723–736.

Westerblad, H., S. Duty, and D.G. Allen. 1993. Intracellular calcium concentration during low-frequency fatigue in isolated single fibers of mouse skeletal muscle. *J. Appl. Physiol.* 75:382–388.

Zhao, M., S. Hollingworth, and S.M. Baylor. 1996. Properties of tri- and tetracarboxylate Ca^{2+} indicators in frog skeletal muscle fibers. *Biophys. J.* 70:896–916.

Zot, H.G., K. Guth, and J.D. Potter. 1986. Fast skeletal muscle skinned fibers and myofibrils reconstituted with N-terminal analogues of troponin C. *J. Biol. Chem.* 261:15883–15890.

Zot, H.G., and J.D. Potter. 1987. Calcium binding and fluorescence measurements of dansylaziridine-labelled troponin C in reconstituted thin filaments. *J. Muscle Res. Cell Motil.* 8:428–436.